25th ABCM International Congress of Mechanical Engineering
October 20-25, 2019, Uberlândia, MG, Brazil

COB-2019-0268
ACOUSTIC CHARACTERIZATION OF THE NOISE GENERATED BY TURBOCHARGERS

Vítor Mourão Hanriot
Colegiado de Graduação em Engenharia de Controle e Automação, Universidade Federal de Minas Gerais, Brazil.
Centro de Tecnologia da Mobilidade, Universidade Federal de Minas Gerais, Brazil.
vhanriot@ufmg.br

Fernanda Dias Troysi
Programa de Pós-Graduação em Engenharia Mecânica, Pontifícia Universidade Católica de Minas Gerais, Brazil.

José Arthur G. S. Teixeira
Ramon Molina Valle
Oscar R. Sandoval
Programa de Pós-Graduação em Engenharia Mecânica, Universidade Federal de Minas Gerais, Brazil.
Centro de Tecnologia da Mobilidade, Universidade Federal de Minas Gerais, Brazil.

Abstract. *Although turbochargers help reducing vehicles pollutant emissions, once compressed air helps in burning less fuel for the same amount of power, they negatively contribute to another problem: noise pollution. Studies about vehicles sound emission have been developed and significant results relating traffic noise and ischemic heart diseases were made, which therefore urges an attention about the noise generated by turbochargers, once this gears can reach high levels of decibels while operating. Thus, it is necessary to characterize the sound intensity generated by turbochargers. This paper presents a method to calculate the intensity generated by turbochargers using a beamformer named Linearly Constrained Minimum Variance, which consists in extracting signals with predetermined angles from the pressure wave signal captured by an array of sensors. The array is composed by two microphones mounted flush to the compressor's axis and the sensors are set outside of the inlet duct. After the acoustic signal decomposition, the sound intensity level in four compressor operational speeds is presented.*

Keywords: *noise pollution, compressor, LCMV beamforming, compressor's noise emission.*

1. INTRODUCTION

A major discussion about vehicle pollutants has been on, since those are one of the biggest agents of world climate change. One-fifth of European Union's total CO_2 emissions are contributed by road transport, 75% originated by passenger cars, which is 20.5% higher than in 1990 (Fontaras *et al.*, 2017) and, according to Woon Jang *et al.* (2014), CO_2 concentration around the globe is above 398 parts per million and this number is getting higher throughout the years. The author described the fossil fuel combustion, highly used in automotive industries for transportation, as the largest human impact on CO_2 emissions.

Many strategies built towards diminishing effects of this vehicle emissions have been developed. One of them is to reduce the amount of fossil fuels used. In Brazil, the use of ethanol is a trend since taxes for manufacturers have been smoothed, which turned ethanol out to be 52% of the fuel consumption (Woon Jang *et al.*, 2014). Another strategy is the use of turbochargers. Commonly used in recent years, turbochargers play an important role in reducing this effects (Kruiswyk, 2012), once compressed air helps in burning less fuel for the same amount of power.

However, atmospheric pollution is not the only negative outcome of vehicle popularization throughout recent years. According to the World Health Organization, noise pollution is considered the second leading environmental hazard. Babisch *et al.* (2005) discussed the correlation between noise and cardiovascular diseases such as high blood pressure and ischemic heart diseases, in which about 2% to 3% of ischemic heart diseases are related to traffic noise. This traffic noise can be harmful when the sound pressure level reaches magnitude of 65 to 70 decibels (dB). Twardella and Ndrepepa (2011) used a meta-analytic methodology to summarize different studies about the correlation between noise traffic and cardiovascular diseases, and this meta-analysis showed that individuals subjected to higher categories of noise have a 15.5% increase of having arterial hypertension and nearly 7% risk of having ischemic heart disease. Fiedler and Zannin (2015), as presented in the Fig. 1, studied the noise intensity in an urban region of Curitiba city in Brazil. The authors

showed that the noise gets higher while it gets closer to the streets, reaching levels of 75 to 80 dB. In the scientific literature it is observed that turbochargers are one of the biggest vehicle noise generators (Figurella *et al.*, 2014; Sundström *et al.*, 2018), thus, the study of a method to determine the acoustic noise emission of this engine component is necessary. Therefore, this paper presents a beamforming methodology to calculate the intensity vector for an acoustic pressure signal of an automotive turbocharger using a two microphone instrumentation.

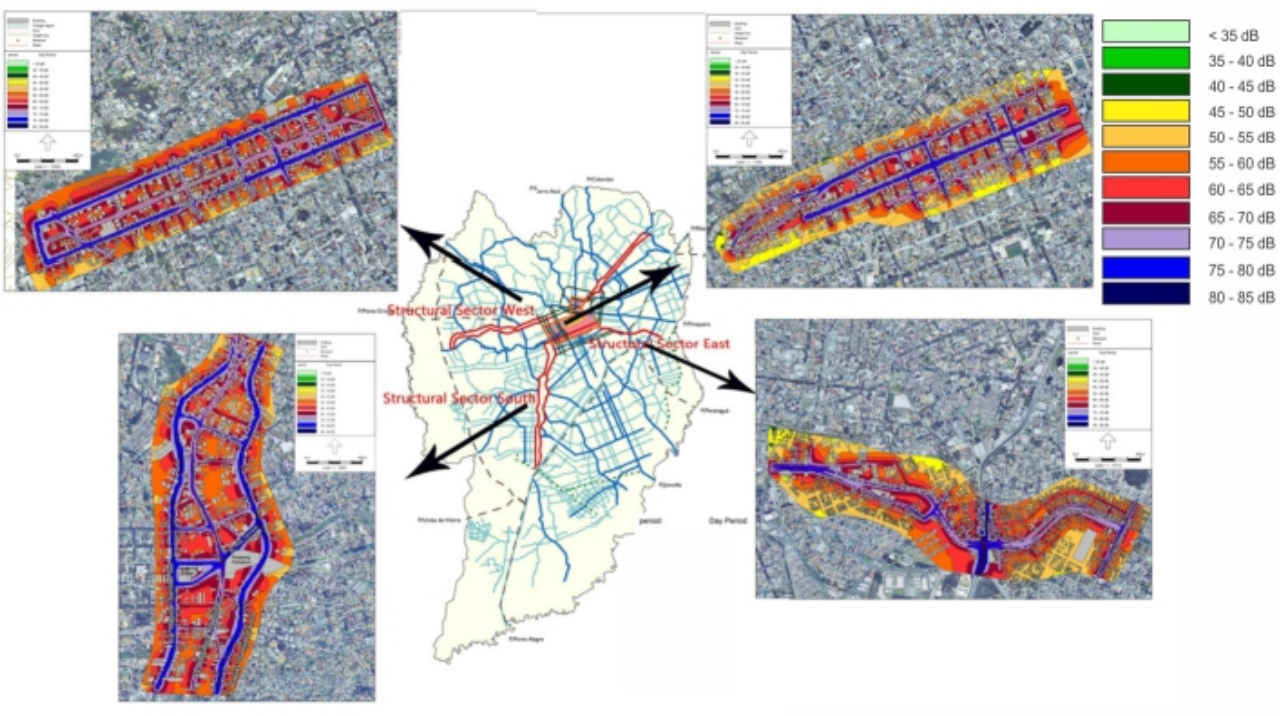

Figure 1: Curitiba noise at streets (Fiedler and Zannin, 2015)

2. METHODOLOGY

2.1 Beamforming decomposition

Beamforming method, presented in the Fig. 2, is a way of decomposing a signal into several signals with different direction angles, each signals multiplied by a weight previously calculated (García Tíscar, 2017). It is an effective method once it isolates the signal by chosen angles, improving the signal accuracy considering that undesirable signals are neglected. It is also effective because the set of sensors allows to collect the same signal from different positions, providing the calculus of the sound intensity level, a vector measurement that is not influenced by the duct geometry (García Tíscar, 2017), otherwise if using only one sensor, the geometry of the duct can not be overlooked. As presented by García Tíscar (2017), the pressure signal $x(t)$ is taken by a linear vector of sensors. This phased array shifts the signal phase by a weight w_n^*, and then forms a plane wave emitted in the θ direction, which can be previously chosen by calculating the respective w_n^*. This technique allows to decompose the pressure signal into downstream and upstream waves, both interesting once these signals summarizes what leaves and enters the compressor (Verdú, 2003).

This method can also be applied by using Fast Fourier Transform ($\mathscr{F}$). Equation 1 shows the Fast Fourier Transform applied for each sensor of the array.

$$\mathbf{X_n} = \mathscr{F}\{\mathbf{x_n}\} \tag{1}$$

Where $\mathbf{x_n}$ represents the matrix of data collected by the sensors.

The Linearly Constrained Minimum Variance (LCMV) is a beamformer method based on the Fast Fourier Transform application for each sensor $x(t)$. It consists in extracting signals with predetermined angles from the acoustic pressure wave signal captured by the sensors (García Tíscar, 2017). By doing that, the signal is spatial filtered so noises and unwanted signals are neglected. In this study, the sound intensity is affected only by the signals radiated in the compressor's inlet duct. Due to it, angles of 90^o and -90^o are the ones to be chosen.

The acoustic signal $x(t)$ taken from the turbocharger's compressor inlet, as shown by the Eq. 2, can be considered as a superposition of the signals of the downstream flow $x^+(t)$ and the upstream flow $x^-(t)$.

$$x(t) = x^+(t) + x^-(t) \tag{2}$$

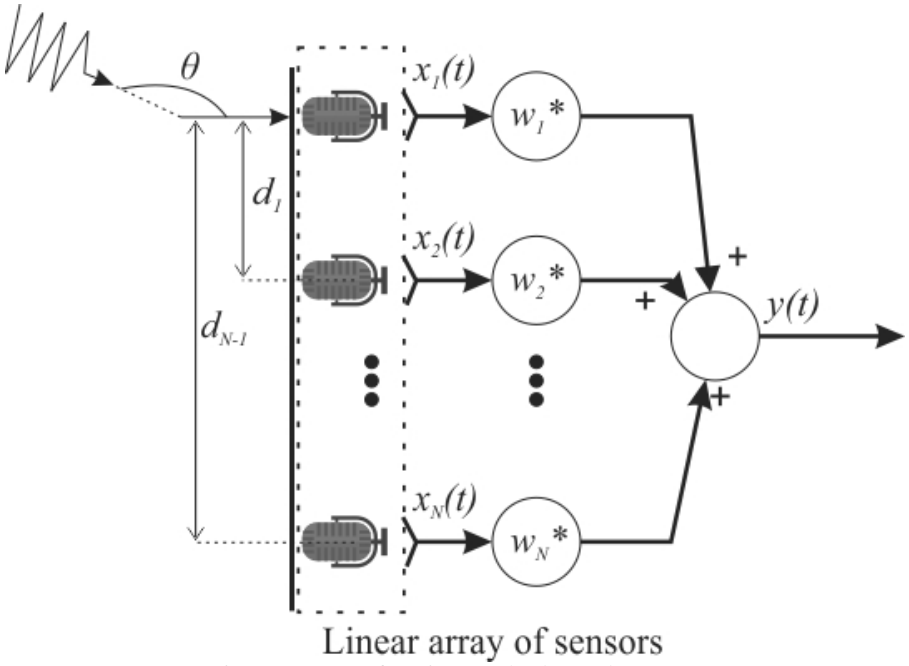

Figure 2: Beamforming method (Verdú, 2003)

By using this decomposition, the sound intensity can be estimated by the Eq. 3.

$$\mathbf{I} = \frac{1}{\rho a}\left(|\mathbf{X}^{+}|^{2}(1+M)^{2} - |\mathbf{X}^{-}|^{2}(1-M)^{2}\right) \tag{3}$$

Where $\mathbf{X}^{+}$ and $\mathbf{X}^{-}$ are the vectors containing the complex spectra of the downstream and upstream wave acoustic pressure determined by Eq. 4 and Eq. 5, respectively. ρ is the mean density of the fluid, a is the fluid speed, M is the mean Mach number and $|\cdot|$ indicates the determinant operator.

$$\mathbf{X}^{+}(f_k) = \mathbf{w}^{+H}\mathbf{X}(f_k); \tag{4}$$

$$\mathbf{X}^{-}(f_k) = \mathbf{w}^{-H}\mathbf{X}(f_k); \tag{5}$$

The remaining equations listed below are calculated for each Fourier frequency f_k of the transformed signal $\mathbf{X}(f_k)$

The matrix of weights $\mathbf{w}$ determined by the Eq. 6 is N×2, where N is the number of sensors used in the experimental test. The first line of the matrix corresponds to the $\mathbf{w}^{+}$ (Eq. 7), while the second corresponds to the $\mathbf{w}^{-}$ (Eq. 8).

$$\mathbf{w} = \left[\sum\nolimits_{x}^{-1}\mathbf{A}^{H}\left[\mathbf{A}^{H}\sum\nolimits_{x}^{-1}\mathbf{A}^{H}\right]^{-1}\right] \tag{6}$$

Where $(\cdot)^{H}$ corresponds to the Hermitian operator, which is equal to its conjugate transpose. $\sum_x$ is the covariance matrix and $\sum_x^{-1}$ is the inverse of the covariance matrix and the constraints matrix $\mathbf{A}$ is determined by the Eq. 9.

$$\mathbf{w}^{+} = \mathbf{w}[1\,0]^{T} \tag{7}$$

$$\mathbf{w}^{-} = \mathbf{w}[0\,1]^{T} \tag{8}$$

$$A = [a^{+}\,a^{-}]^{T} \tag{9}$$

Where the direction vectors for the downstream $\mathbf{a}^{+}$ and upstream $\mathbf{a}^{-}$ waves are calculated by the Eqs. 10 and 11.

$$\mathbf{a}^{+} = \mathbf{a}(-90^{o}) = [1, e^{j\beta^{+}d_s}, e^{j\beta^{+}2d_s}, e^{j\beta^{+}3d_s}, \cdots, e^{j\beta^{+}Nd_s}]^{T} \tag{10}$$

$$\mathbf{a}^{-} = \mathbf{a}(90^{o}) = [1, e^{-j\beta^{-}d_s}, e^{-j\beta^{-}2d_s}, e^{-j\beta^{-}3d_s}, \cdots, e^{-j\beta^{-}Nd_s}]^{T} \tag{11}$$

Where d_s is the distance between the sensors. β^{+} and β^{-} are determined by the Eq. 12 and the Eq. 13 respectively.

$$\beta^{+} = \frac{k + \alpha(1-j)}{1+M} \tag{12}$$

$$\beta^{-} = \frac{k + \alpha(1-j)}{1-M} \tag{13}$$

In which $k = \omega/c, \omega = 2\pi f_k$ and α is the viscothermal attenuation coefficient described by the Eq. 14.

$$\alpha = \frac{1}{ra}\left(\frac{\nu\omega}{2}\right)^{\frac{1}{2}}\left[1 - (\gamma-1)Pr^{-0.5}\right] \tag{14}$$

Where r is the duct radius, a the speed of sound constant and ν is the kinematic viscosity and Pr is the Prandtl number. Finally the Sound Intensity Level (SIL) and the total Sound Intensity Level (SIL_T) are calculated by following Eq. 15 and Eq. 16 respectively.

$$SIL(i) = 10log_{10}\left(\frac{|I(i)|}{10^{-12}}\right) \tag{15}$$

$$SIL_T = 10log_{10}\left(\sum_{i=1}^{m}\frac{|I(i)|}{10^{-12}}\right) \tag{16}$$

Where m is the length of the sound intensity divided by 2.

The frequency range of the acoustic energy must be settled. In order to attend the Nyquist theorem, the wave's time of travel T_s described by Eq. 17 dependent on the distance between the microphones d_s settles the signals frequency of $f_d = \frac{1}{T_s}$. Nyquist-Shannon sampling theorem establishes the sampling frequency as half of the experimental frequency, described in Eq. 18.

$$T_s = \frac{d_s}{a} \tag{17}$$

$$f_s \leq \frac{a}{2d_s} \tag{18}$$

Whereas Nyquist Theorem considers the sampling frequency, the assumption of one-dimensional-only waves of the acoustic method settles limits to the frequency range. According to Verdú (2003), modes of higher order start to propagate beyond a cut-off frequency determined by Eq. 19, hence the assumption of planar waves travelling alongside the pipe in a one dimensional movement must be considered within the range below the cut-off frequency determined.

$$f_c = 1.84\frac{a}{\pi D}\sqrt{1-M^2} \tag{19}$$

where a is the sound speed, D is the duct diameter and M is the mean Mach number.

Once the Power Spectra Density is collected, it is possible to assess its features based on the literature.

2.2 Turbochargers noise characterization

In order to characterize the most relevant noises emitted by the compressor, the acoustic emission of a moving source must be settled. Hence, Ffwocs Williams-Hawkings model described by Eq. 20 is considered, as it is an acoustic analogy derived from the Lightill-Curle theory of aerodynamic sound to include arbitrary convective motion, as stated at (Williams and Hawkings, 1969). In this acoustic analogy, the right-handed terms are nonlinear terms commonly related to sound sources, providing the computation of far-field noise induced by the flow of a fluid in a three-dimensional ducted fan geometry system (Orselli *et al.*, 2018). In Eq. 20, u_i is the fluid component in the x_i direction, u_n is the fluid velocity normal to the surface, v_i are the surface velocity components in in the x_i direction, v_n is the surface velocity component normal to the surface, $\delta(f)$ is the Dirac delta function and $H(f)$ is the Heaviside function. p' is the sound pressure at far field, n_i is the unit normal vector, a_0 is the far-field sound speed, T_{ij} is the Lightill stress tensor and P_{ij} is the compressive stress tensor.

Åbom (2014) characterizes the sound emitted by a moving source in three distributions: monopoles (first term at the right hand side of Eq. 20), dipoles (second term at the right hand side of Eq. 20) and quadrupoles (third term at the right hand side of Eq. 20). Monopoles noises are an outcome of volume displacement, whereas dipole noises are related to fluctuating pressures and quadrupoles result from unsteady Reynolds transport of momentum. In the compressor, the main noises are the aero-acoustic ones, related to reflection and transmission of pulses and high-frequency noises resulted from high speeds.

$$\frac{1}{{a_o}^2}\frac{\partial^2 p'}{\partial t^2} - \nabla^2 p' = \frac{\partial}{\partial t}([\rho_o v_n + \rho(u_n - v_n)]\delta(f)) - \frac{\partial}{\partial x_i}([P_{ij}n_j + \rho u_i(u_n - v_n)]\delta(f)) + \frac{\partial^2}{\partial x_i \partial x_j}(T_{ij}H(f)) \quad (20)$$

Studies towards these aero-acoustic turbocharger acoustic emissions have been already discussed on the literature. García Tíscar (2017) distinguishes these noises by internal flow noise, typically seized by sensors placed inside the compressor housing in both inlet and outlet ducts, and radiated noises, external measurements usually made by microphones. The most common and specified noises in the literature regarding aerodynamics and the flow generated sound in the system are the Buzz-saw Noise, related to engine high-power operations when supersonic fans produce tones harmonically synchronized with the engine's shaft speed, which is generated by rotating shock waves (McAlpine *et al.*, 2012), the tonal noise at Blade Passing Frequency (BPF), an outcome of the compressor's blades subjected to periodic turbulence which causes noise emission at these frequencies (Eq. 21 describes the harmonics generated by this phenomenon, where B is the number of main rotor blades and N is the speed of the compressor), and the Tip Clearance Noise (TCN), a narrow-band noise generated by the secondary flow created in the gap between the compressor casing and the impeller blade tips which presents itself typically at frequencies of about half of the BPF (Galindo *et al.*, 2015). Åbom (2014) mentions the Rotating Stall noise, a broadband peak associated with flow separation at subsonic compressor speeds, and García Tíscar (2017) also mentions a general broadband type noise related to operations close to surge known as whoosh noise. The Buzz-saw noise is of monopole distribution, whereas BPF, TCN and rotating stall are of dipole distribution (Åbom, 2014).

$$BPF = B \cdot \frac{N}{60} \quad (21)$$

3. EXPERIMENTAL SETUP

The hot gas flow test rig used to develop the experimental test has the following characteristics:

- Two screw compressors with a maximum mass flow capacity of 0.6 kg s^{-1}, at a maximum discharging pressure of 400 kPa which feed a storage tank with 5 m^3 air capacity. This compressed air is conducted to the turbine and its mass flow rate is controlled by changing the opening of a pneumatic discharge valve.
- Compressor mass flow is measured by a turbine-typed instrument. The exhaust gases that provides energy to run the turbocharger compressor have a controlled temperature of 400 ^{o}C.
- The turbocharger compressor speed is measured using an emitter/receiver sensor, which uses a laser beam to transform the frequency of the received pulses into an analog signal proportional to the speed. An independent lubrication system is installed with a control inlet oil temperature and pressure strategy. Inlet and outlet temperatures are measured using type K thermocouples and pressure is measured with a piezoresistive transmitters. All sensor in the installation have been previously calibrated.
- Two microphones PCB Piezotronics are set in the compressor's inlet, capturing the acoustic pressure signal coming out of the compressor. This microphones are shown in Fig. 3.
- The signal captured is then processed by a program in the LabVIEW software. This software generates the signal data which is then treated by a MATLAB program which follows the methodology shown previously.

In this paper, a centrifugal compressor of a turbocharger Garrett TA31 is tested. Regarding that the maximum speed of this turbocharger is 130 krpm, four different speeds of 40 krpm, 60 krpm, 80 krpm and 100 krpm are tested and for each speed, six different points are collected by varying the compressor mass flow until it is close to the surge boundary by means of an Back-pressure Valve placed in the compressor's outlet.

4. RESULTS AND DISCUSSION

The sound intensity presented in the Fig. 4 is the result of different compressor mass flows at 40 krpm, 60 krpm, 80 krpm and 100 krpm. Six operational points for each speed were tested, for 100% (Op1), 75% (Op2), 50% (Op3), 40% (Op4), 30% (Op5) of the Back-pressure Valve Opening and the opening where the compressor is subjected to surge conditions (Op6), which are 83%, 78%, 75% and 72% at 40 krpm, 60 krpm, 80 krpm and 100 krpm, respectively.

It is noticeable that the amplitude increases with the increase of the compressor speed. The amplitude also grows when closing the valve, once mass flow slump provides an increase in the fluid's speed, what thereupon contributes to the rise of sound emitted by the compressor. Whoosh noise, a broadband noise starting at around 2.5 kHz is seen specially for speeds of 60 krpm, 80 krpm and 100 krpm. Considering that the compressor tested has six blades, BPF harmonics are not visible since those are at frequencies beyond the cut-off frequency determined by both the Nyquist theorem and the one

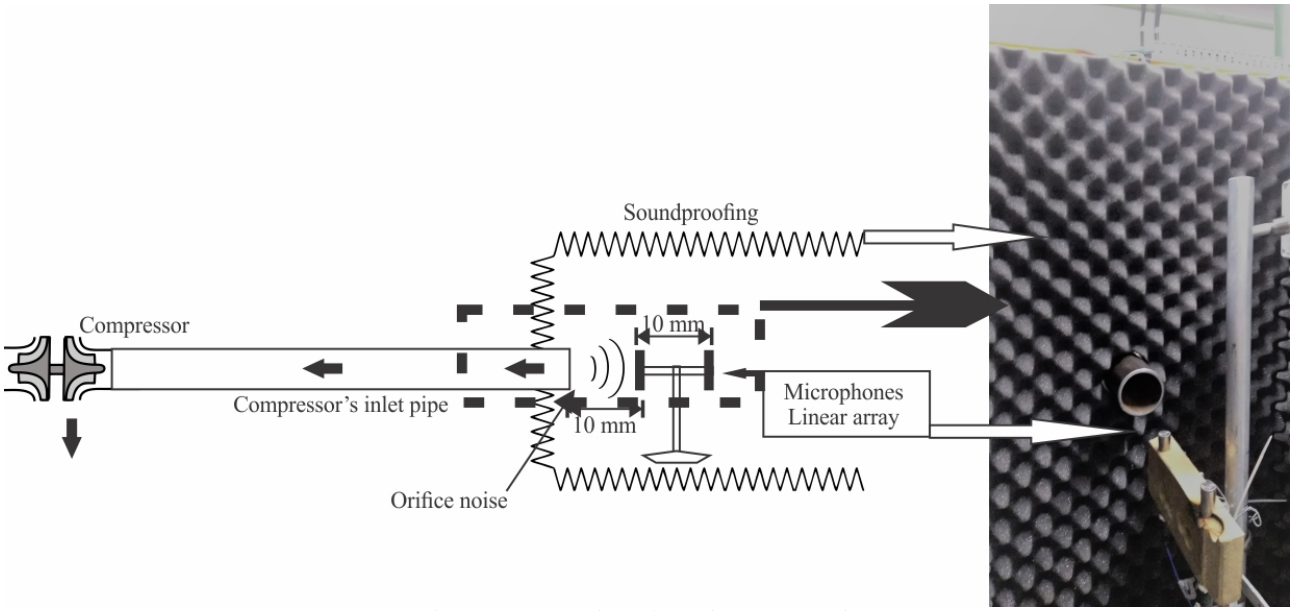

Figure 3: Two microphone instrumentation

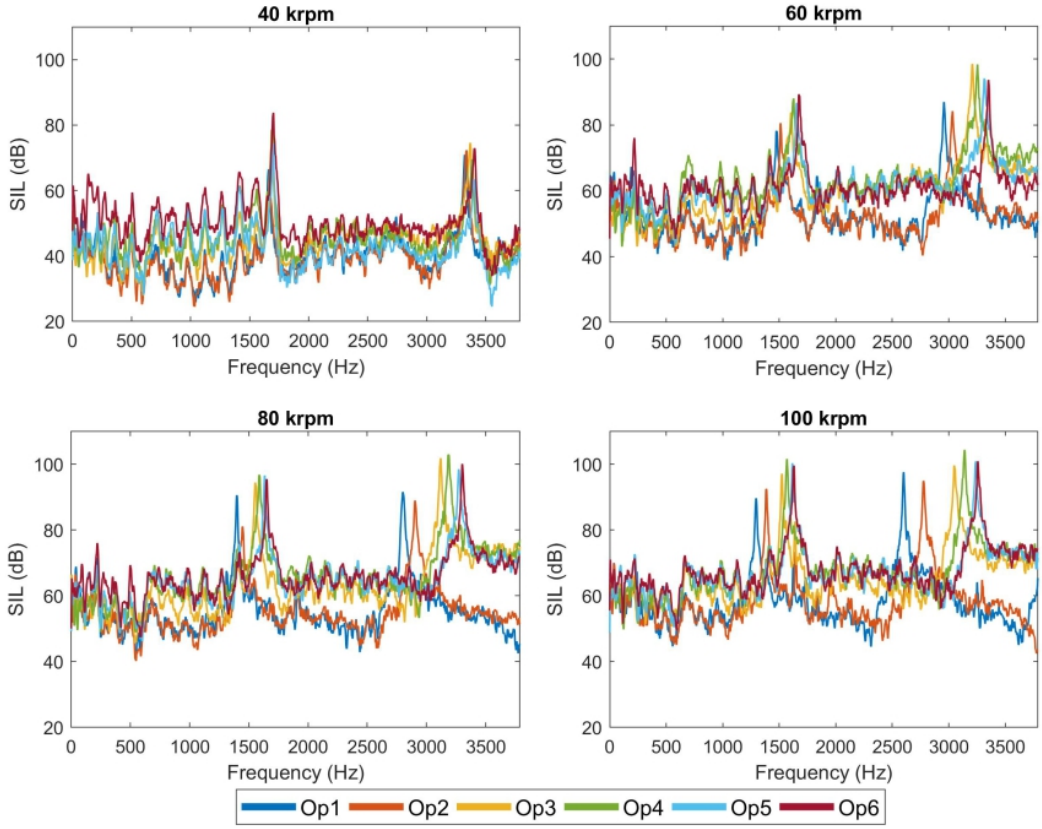

Figure 4: Sound Intensity Level (SIL) for six operational points at 40 krpm (top left), 60 krpm (top right), 80 krpm (bottom left) and 100 krpm (bottom right)

mode wave propagation assumption, which is 3788 Hz. While for speeds such as 40 krpm all of the operational points present a similar shape, for speeds specially of 80 krpm and 100 krpm Op1 and Op2 present a deviance of approximately 15 dB at higher frequencies. Two harmonics can also be seen at all speeds, the first peak around 1.7 kHz and the second peak around 3.3 kHz. Once these harmonics show up at almost fixed frequencies, they are not related to the increase of the compressor speed. The literature does not present an exact explanation of these peaks, although harmonics peaks at lower frequencies due to tonal noise phenomena produced by the engine are discussed (García Tíscar, 2017). In this study, though, the compressor does not work aside an engine, therefore it is assumed that these peaks are related to the air flow

distribution along the test bench.

Fig. 5 shows a comparison between speeds at each operational point tested. It can be seen that for all the percentages of Back-pressure Valve Opening SIL is proportionally related to the compressor speed. It is also clear that as the mass flow varies towards the surge limit, specially after 75% of Back-pressure Valve Opening, SIL at speeds of 60 krpm, 80 krpm and 100 krpm become similar. SIL at 40 krpm maintains its shape while varying the valve opening, which can also be seen at the top left figure of Fig. 4. Because of that, at operations close to surge, specially for Op4 and Op5, there is a 30 dB difference between SIL at 40 krpm and SIL at other speeds. This is due to the temperature increase at high speeds, which increases the noise generated by the compressor.

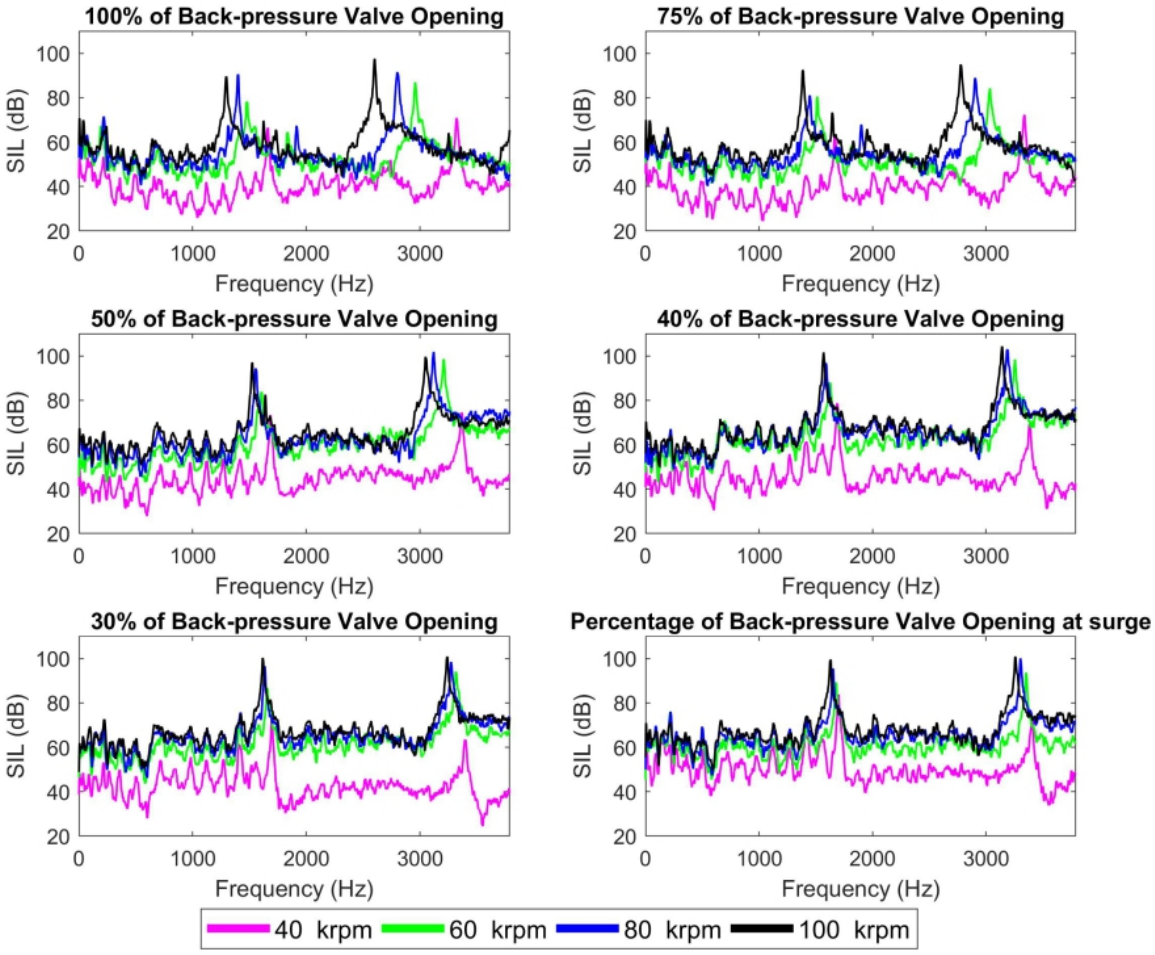

Figure 5: Sound Intensity Level for 40 krpm, 60 krpm, 80 krpm and 100 krpm at Op1 (top left), Op2 (top right), Op3 (middle left corner), Op4 (middle right corner), Op5 (bottom left), Op6 (bottom right)

5. CONCLUSIONS

Two microphones set in the orifice of the compressor's inlet were used to capture acoustic waves at six operational points for four different speeds (40 krpm, 60 krpm, 80 krpm and 100 krpm). The beamforming method was used to determine the Sound Intensity Level of the signals, which led to a characterization of common noises described by the literature.

SIL levels reached values over 100 dB, higher than the levels in which human diseases start to correlate with acoustic noise emissions. Therefore the compressor must be considered when strategies aiming to reduce noise emitted by vehicles are developed. The beamforming method appears as a valid method to quantify noise levels and is also useful to the development of methods that build intensity acoustic maps, as the sound intensity estimated by the beamforming can be used to calculate the sound intensity level for each operational point.

The acoustic quantification of turbochargers lead to a characterization of commonly described noises in the literature. When these noises are well known, an intake attenuation system can be developed regarding their appearance.

6. REFERENCES

Babisch, W., Beule, B., Schust, M., Kersten, N. and Ising, H., 2005. "Traffic Noise and Risk of Myocardial Infarction". *Epidemiology*, Vol. 16, No. 1, pp. 33–40. ISSN 1044-3983. doi:10.1097/01.ede.0000147104.84424.24.

Fiedler, P.E.K. and Zannin, P.H.T., 2015. "Evaluation of noise pollution in urban traffic hubs-Noise maps and measurements". *Environmental Impact Assessment Review*, Vol. 51, pp. 1–9. ISSN 01959255. doi:10.1016/j.eiar.2014.09.014.

Figurella, N., Dehner, R., Selamet, A., Tallio, K., Miazgowicz, K. and Wade, R., 2014. "Noise at the mid to high flow range of a turbocharger compressor". *Noise Control Engineering Journal*, Vol. 62, No. 5, pp. 306–312. ISSN 07362501. doi:10.3397/1/376229.

Fontaras, G., Zacharof, N.G. and Ciuffo, B., 2017. "Fuel consumption and CO2 emissions from passenger cars in Europe - Laboratory versus real-world emissions". *Progress in Energy and Combustion Science*, Vol. 60, pp. 97–131. ISSN 0360-1285. doi:10.1016/J.PECS.2016.12.004.

Galindo, J., Tiseira, A., Navarro, R. and López, M., 2015. "Influence of tip clearance on flow behavior and noise generation of centrifugal compressors in near-surge conditions". *International Journal of Heat and Fluid Flow*, Vol. 52, pp. 129–139. ISSN 0142-727X. doi:10.1016/J.IJHEATFLUIDFLOW.2014.12.004.

García Tíscar, J., 2017. *Experiments on turbocharger compressor acoustics*. Ph.D. thesis, Universitat Politècnica de València, Valencia (Spain). doi:10.4995/Thesis/10251/79552.

Kruiswyk, R., 2012. "The role of turbocompound in the era of emissions reduction". In *10th International Conference on Turbochargers and Turbocharging*, Elsevier, pp. 269–280. doi:10.1533/9780857096135.5.269.

McAlpine, A., Schwaller, P., Fisher, M. and Tester, B., 2012. ""Buzz-saw" noise: Prediction of the rotor-alone pressure field". *Journal of Sound and Vibration*, Vol. 331, No. 22, pp. 4901–4918. ISSN 0022460X. doi:10.1016/j.jsv.2012.06.009.

Orselli, R.M., Carmo, B.S. and Queiroz, R.L., 2018. "Noise predictions of the advanced noise control fan model using lattice Boltzmann method and Ffowcs Williams-Hawkings analogy". *Journal of the Brazilian Society of Mechanical Sciences and Engineering*, Vol. 40, No. 1, p. 34. ISSN 1678-5878. doi:10.1007/s40430-018-0982-2.

Åbom, M., 2014. "Turbocompressor Aeroacoustics - Public Technical Course 1". Technical report, KTH Royal Institute of Technology.

Sundström, E., Semlitsch, B. and Mihăescu, M., 2018. "Acoustic signature of flow instabilities in radial compressors". *Journal of Sound and Vibration*, Vol. 434, pp. 221–236. ISSN 0022460X. doi:10.1016/j.jsv.2018.07.040.

Twardella, D. and Ndrepepa, A., 2011. "Relationship between noise annoyance from road traffic noise and cardiovascular diseases: A meta-analysis". *Noise and Health*, Vol. 13, No. 52, p. 251. ISSN 1463-1741. doi:10.4103/1463-1741.80163.

Verdú, I., 2003. *Contribución al estudio y caracterización de la generación de ruido de flujo en el sistema de escape.* Ph.D. thesis, Universitat Politècnica de València, Valencia (Spain). doi:10.4995/Thesis/10251/2622.

Williams, J.E.F. and Hawkings, D.L., 1969. "Sound Generation by Turbulence and Surfaces in Arbitrary Motion". *Philosophical Transactions of the Royal Society A: Mathematical, Physical and Engineering Sciences*, Vol. 264, No. 1151, pp. 321–342. ISSN 1364-503X. doi:10.1098/rsta.1969.0031.

Woon Jang, Y., Park, I.S., Ha, S.S., Jang, S.H., Chung, K.W., Lee, G., Kim, W.H., Choi, Y.J. and Cho, C.H., 2014. "Preliminary analysis of the development of the Carbon Tracker system in Latin America and the Caribbean". *Atmósfera*, Vol. 27, No. 1, pp. 61–76. ISSN 01876236. doi:10.1016/S0187-6236(14)71101-4.